A survey of the natural remanent magnetization and magnetic susceptibility of Apollo whole rocks

Camille Lepaulard, Jérôme Gattacceca, Minoru Uehara, Pierre Rochette, Yoann Quesnel, Robert Macke, S.J. Walter Kiefer

A survey of the natural remanent magnetization and magnetic susceptibility of Apollo whole rocks

Camille Lepaulard[1], Jérôme Gattacceca[1], Minoru Uehara[1], Pierre Rochette[1], Yoann Quesnel[1], Robert J. Macke[2], S.J. Walter Kiefer[3]

[1]Aix Marseille University, CNRS, IRD, Coll France, INRA, CEREGE, Aix-en-Provence, France

[2]Vatican Observatory, Vatican City-State

[3]Lunar and Planetary Institute, Houston, Texas, USA

Corresponding author: Camille Lepaulard

E-mail address: lepaulard@cerege.fr

Postal address: CEREGE, Technopôle environnement, Arbois-Méditerannée BP80

13545 Aix-en-Provence, CEDEX 04, FRANCE

Key words

Apollo samples; remanence; paleomagnetism; magnetic susceptibility

Abstract

Magnetic properties of lunar rocks may help understand the evolution of the past magnetic field of the Moon. However, these properties are often measured on small subsamples, which may not be representative of the bulk lunar rocks. In this study, a rough magnetic characterization of a large fraction of the Apollo collection was performed using non-destructive methods to determine the paleomagnetic signal, with a focus on large samples (mean mass 500 g). The natural remanent magnetization of 123 Apollo samples and the magnetic susceptibility of 154 Apollo samples were measured in the Apollo storage vault at the Lunar Sample Laboratory Facility in Houston. Magnetic susceptibility is strongly controlled by lithology and is clearly enhanced by impact processing and associated incorporation of meteoritic metal. The natural remanent magnetization is lower by a factor of ~3 than that measured by other researchers on small laboratory samples, suggesting magnetic contamination during small-sample preparation or handling, or directional heterogeneity in remanence within large samples. The laboratory measurements were conducted on subsamples of the same sample measured in this study. The ratio of natural remanence

magnetization to magnetic susceptibility may be used as selection tool for further paleomagnetic study. It is a crude paleointensity proxy and its overall temporal evolution is coherent with the existence of a high magnetic field from ~4 Ga to 3.5 Ga and a subsequent weaker field epoch as previously defined in the literature. Our data also raise the possibility that the intensity of the paleomagnetic field during the high field epoch may have been more variable and lower on average than previously suggested.

1. Introduction

The existence of past or present magnetic fields on the Moon was a matter of debate before lunar exploration started, as it was one of the key factors in distinguishing between a "hot Moon" versus a "cold Moon" model. Early orbital magnetic measurements by Luna 10 (*Dolginov et al*., 1966) and Explorer 35 (*Sonett et al*., 1967) satellites were only able to determine upper limits of the magnetic fields in the vicinity of the Moon, indicating that any lunar fields would be much weaker than that of the Earth, and suggesting a non-magnetic body. However, the Apollo orbital and surface magnetometers revealed patches of significant field due to crustal remanence. The paleomagnetic study of Apollo samples suggested the record of past strong (i.e., Earth-like) magnetic fields at the surface of the Moon (e.g., *Fuller et al*., 1987), besides the particular difficulties linked with retrieving reliable paleointensities in metal-bearing rocks (e.g. *Lawrence et al*. 2008).

Analysis of Apollo samples establishes constraints on the temporal evolution of the lunar magnetic field. This evolution reveals two main magnetic epochs: a high-field epoch with paleointensities of several tens of μT between about 4.25 and 3.56 Ga (*Garrick-Bethell et al*., 2009, 2017; *Cournède et al*., 2012; *Shea et al.*, 2012; *Tikoo et al*., 2012a; *Suavet et al*., 2013); followed by a weak-field epoch with paleointensities below 10 μT (*Tikoo et al*., 2014) and down to < 4 μT after 3.19 Ga (*Tikoo et al*., 2014, 2017; *Weiss et al*., 2014; *Buz et al*., 2015).

In part because the age distribution of Mare basalts peaks between 3.8 and 3.3 Ga (*Hiesinger et al., 2011*), the high-field epoch is rather well constrained, with around 60 studied samples (*Cisowski et al*., 1983; *Weiss et al*., 2014). However, paleointensities up to 100 μT are at odds with dynamo models that predict much lower surface fields (*Dwyer et al*., 2011; *Le Bars et al*., 2011; *Laneuville et al*., 2014; *Evans et al*. 2017). Also, some samples may indicate paleointensities < 10 μT during this high-field epoch (*Fuller et Cisowski*, 1987), raising the possibility of a highly variable or intermittent dynamo (*Evans et al*., 2017). Further

data from this high-field epoch is thus needed to strengthen the robustness of the high paleofields claims, and test the possibility of an intermittent or highly variable dynamo.

The weak-field epoch is defined as the period of decline of the field intensity, down to the present day situation with no internally generated field (*Fuller and Cisowski*, 1987; *Tikoo et al*., 2014). This epoch is constrained by 30 paleointensity estimates (*Cisowski et al*., 1983; *Weiss et al*., 2014; *Tikoo et al*., 2017; *Wang et al*., 2017). Recent analyses of young samples reveal surface field intensities from 5 ± 2 μT (~2.5-1 Ga, *Tikoo et al*., 2017) to <1 μT (~1 Ga, *Wang et al.*, 2017). These results could be explained by the persistence of a weak dynamo powered by core crystallization and mantle precession from 2.5 to 1 Ga (*Tikoo et al*., 2017). Numerical modeling studies show that core convection could indeed generate surface fields of 2 μT until up to 200 Ma (*Evans et al*., 2017). The field evolution over the weak-field epoch is rather poorly defined, especially between 3 and 2 Ga, a time interval where both basalts and regolith breccias are rare (*Hiesinger et al*., 2011; *Fagan et al*., 2014).

So far, fewer than 70 small (usually well below 1 g) samples of Apollo rocks have been studied for paleomagnetism, compared to a total of 1402 rock samples available in the Apollo collection (this latter number is a personal communication by Ryan Zeigler). The aim of this study is to obtain a rough estimate of the paleomagnetic potential of a larger fraction of the Apollo rock collection (fraction that span the entire age range that the lunar dynamo has been previously investigated) using non-destructive methods. We measured the natural remanent magnetization (NRM) and the magnetic susceptibility (χ) of whole Apollo samples. These data increase the database of lunar rocks magnetic properties. The measurement of these two properties on the same sample also allows a qualitative assessment of the paleomagnetic potential of these samples. These methods, in addition to being non-destructive, are fast, easy to implement and allow us to measure whole samples. The NRM intensity is a crude indication of whether a rock can be targeted for paleomagnetic study. χ is a proxy for the metal content. The ratio between NRM and χ can be viewed as a crude proxy for the intensity of the paleofield recorded by a rock, enabling the selection of samples for detailed laboratory demagnetization follow-up studies that address specific questions (timing of the dynamo, maximum field recognized in the weak-field epoch, etc). A high NRM/χ may also be an indication of suitable paleomagnetic intrinsic properties for laboratory follow-up studies. Finally, these analyses increase the database of lunar rock magnetic properties for the purposes of modeling the lunar crustal magnetic field (e.g., *Oliveira et al*. 2017).

2. Samples and methods

2.1 Samples

We studied 161 Apollo samples with a focus on large samples (mean mass 497 g, median mass 232 g, mass range 21 to 4688 g, see Table S1). This is much larger than the typical size of specimens used in most previous studies, which were well below 1g (see section S2 in Supplementary material). Of the 161 samples in this study, only 28 had been studied previously for remanent magnetization (samples in literature were measured using a squid magnetometer and with a mean mass of 1 g), and only 37 for magnetic properties. We measured the natural remanent magnetization of 123 samples, the magnetic susceptibility of 154 samples, and 119 samples for which both properties were measured. All specimens in this survey were single coherent bulk samples. We studied basalts, anorthosites, norites, and different types of breccias, spanning the Apollo 11, 12, 14, 15, 16 and 17 landing sites. In the following, a simplified lithological classification of lunar rocks is used (*Heiken and al*., 1991). Breccias are classified into three categories: impact melt breccia (IMB) with clasts set in a melt matrix, dimict breccia (DB) with two distinct lithologies (usually anorthosite and melt rock) and regolith breccia that represent lithified regolith. The other lithologies are impact melt rocks (IMR), basalts, and feldspathic rocks from the lunar highlands (norites, troctolites, anorthosites).

2.2 Methods

All measurements were performed directly in the Apollo storage vault at the Lunar Sample Laboratory Facility (LSLF) at Johnson Space Center (JSC), NASA, Houston. A specific susceptibility meter and a spinner magnetometer were used to be assembled in the LSLF and which satisfy curatorial constraints.

The samples were left in their original packaging for this study. Sample packaging varied from sample to sample. Samples kept in steel containers could not be studied. We measured those stored in Teflon bags, aluminum containers, or a combination of both. Prior to measurements, the samples were placed at the center of a hollow cubic sample holder made of acrylic plastic. They were maintained in place using padding material made of acrylic and Teflon.

The magnetometer and associated data processing methods are described in *Uehara et al*. (2017). The errors associated with the NRM measurements provided in section S1, Table S1, are based on the departure of the measured signal from that of the signal from an ideal dipole (*Uehara et al*., 2017). We validated only samples that fit a dipole source to better than 20% (see discussion in *Uehara et al*., 2017). We did not obtain a satisfactory measurement for

24 samples, either because the magnetization was too low or because the measured signal departed too much from the signal generated by a centered dipole (samples noted with † in the Table S1). These 24 samples range in mass from 24.5 to 1444 g and do not correlate with lithology or size. We did not measure NRMs for 14 samples that consisted of multiple small pieces in a single container (samples noted — in Table S1 in Supplementary material).

The susceptibility meter is described in section S3 in Supplementary material. It consists of an acrylic cylindrical body with two inducing coils and a Hall probe to measure the sum of the alternating inducing and induced fields (Figures S2 and S3 in Supplementary materials). The peak inducing field was 30 $\mu T_{p\text{-}p}$, with absolutely no effect on the paleomagnetic signal, and its frequency was at 5 Hz. This low frequency limits eddy currents in metal and thus enables measurements of samples wrapped in aluminum foils or encapsulated in aluminum containers. This susceptibility meter can accommodate samples as large as 8000 cm^3, corresponding to 20 x 20 x 20 cm sample capsule (which could correspond to a 4.5 kg mass sample). Measurements are based on the assumption that samples are perfectly centered in the instrument. The method of the calculation of the uncertainty on our magnetic susceptibility results is detailed in section S3 in Supplementary material. To limit errors from sample geometric offset and/or anisometric sample shape, we measured the susceptibility in two to three orthogonal positions and used the average result. Magnetic anisotropy of lunar rocks is at most a few percent (e.g., *Rochette et al*., 2010; *Cournède et al.* 2012) and is neglected in this study. The magnetic susceptibility for 41 samples was also measured using a commercial susceptibility meter MS2 from Bartington equipped with a MS2C coil. This coil, with internal diameter of 12 cm, is designed for measurement of cores and was calibrated for discrete samples against a KLY2 large volume kappabridge. The calibration and procedure is provided in section S4 in Supplementary material. Like during the calibration procedure, the measurements were performed along three orthogonal positions and averaged, not so much to account for the weak magnetic anisotropy of lunar rocks, but to account for the effect of sample anisometry on the measurements. For samples measured with both instruments (MS2 and our susceptibility meter), the results compare well, with of coefficient of correlation R^2 = 0.98 and a slope of 1.03 (see section S5 in Supplementary material).

3 Results and discussion

3.1. Magnetic properties and lithology

The NRM intensity spreads over two orders of magnitude (S1, Table S1) and shows a strong lithological dependence, in ascending order of NRM: feldspathic rocks, basalts, breccias and regolith breccia (Figure 1a, Table 1). This corroborates previous results, although on a much larger dataset. Magnetic susceptibility is also lithology-dependent, with impact-processed rocks being more magnetic (i.e., higher NRM and χ) (Figure 1b). This confirms that lunar impact processes are the main factors controlling the amount of ferromagnetic minerals in lunar rocks, with a magnetic enhancement due to incorporation of meteoritic metal (e.g., *Rochette et al*., 2010).

3.2.Comparison with other measurements

The NRM and the magnetic susceptibility values averaged by lithology are given in Table 1, both for this study and for literature data. The literature dataset consists of 109 NRM estimates (from 61 different Apollo rocks), and 105 susceptibility estimates (from 73 different Apollo rocks). A comparison of both datasets shows that the NRM intensities are larger by an average factor of ~2.7 in small sample studies (Figure 2a). This discrepancy (slope of 2.74 and R^2=0.84) is evidence of the NRM directional heterogeneity within some lunar rocks and/or of possible magnetic contamination of small samples during preparation and handling. The two datasets provide similar values for the susceptibility (R^2= 0.90) with a slope of 0.66 (Figure 2b). Standard deviations in the literature data are generally higher than in ours, except for regolith breccias, indicating small-scale heterogeneities in metal content.

For the subset of samples that were previously studied in the literature (section S6, Table S2 in Supplementary material), we compare our NRM measurements on large samples with the laboratory measurements performed on small subsamples of the same rocks (Figure 3). One sample, 15015 is not used due to anomalous result in literature (Table S2). The results of our bulk sample study show a R^2= 0.52. It is noteworthy that when several measurements are available in the literature, there is a large scatter between measurements (with a relative variation from 6% to 163%, 56% in average). This scatter is not due to analytical uncertainties that are small compared to magnetic moments, both in this study and in previous studies. Indeed, basalts have a better correlation (R^2=0.91) than impact melt breccias (R^2=0.18). This is rather further evidence of small-scale heterogeneity of NRM, attributed to lithological heterogeneities (illustrated in section S2), with heterogeneous distribution of metallic iron, especially in breccias. It can indicate too the presence, in the same rock, of lithologies that have recorded contrasting paleofields. Overall, the NRM is higher for small

samples than large samples (see also Table 1), indicating possible magnetic contamination during small samples preparation or handing, or heterogeneous directions of NRM within a large sample.

Our susceptibility data for the large samples and the small subsamples in the literature data (Figure 4) are also correlated (R^2 = 0.69). Impact melt breccia and regolith breccia, shows the best correlation with R^2 of 0.74 and 0.87, respectively. Regolith breccia 60255 and two impact melt breccia (72275 and 77135) are not used due to anomalous result in literature but these results are in Table S2. Feldspathic rocks show the largest discrepancy, our values being up to of 2 orders of magnitude larger than literature data. It is noteworthy that there is a large scatter in literature data (S5, in Table S2) for multiple measurements of subsamples from the same rock, especially for impact melt breccia and impact melt rocks with coefficient of variation of 43% and 59% respectively. Again, small-scale lithological heterogeneities can account for these variations, especially in smaller samples. For feldspathic rocks, the larger whole rock susceptibility may be due to the fact that these rocks often have a coating of melted or regolithic material and that this coating, enriched in metal, was avoided in the subsampling. As an example, samples 65315 and 60215 had diamagnetic χ values of -1.4×10^{-9} $m^3.kg^{-1}$ and -5.4×10^{-9} $m^3.kg^{-1}$, respectively, in the small sample study of *Cournède et al.* (2012) and 20×10^{-9} $m^3.kg^{-1}$ and 228×10^{-9} $m^3.kg^{-1}$, respectively, in this study.

In Figure 5, we compare our susceptibility results with measurements performed at JSC on another set of large samples (mean mass 19.8 g) from the returned sample collection (*Macke et al*., 2014). These measurements were performed using a SM30 instrument calibrated following *Gattacceca et al.* (2004) and are provided in section S7, Table S3. The coefficient of correlation of 0.70, together with a slope of 0.998 between the two independent dataset confirm that the scatter observed between our measurements and the small sample laboratory measurements is due to the intrinsic properties of lunar rocks (mostly small scale heterogeneities) rather than instrumental issues. Still returned samples yield on average lower values than the whole rocks, again suggesting the possible effect of regolith contamination of the surface of whole rocks. It is also possible that measurements using the SM30 contact probe are underestimated because they are sensitive to the surface roughness of the samples and were calibrated for smooth pebble shaped samples (*Gattacceca et al*., 2004).

3.3. Paleomagnetic potential of this dataset

The ratio of NRM to magnetic susceptibility, noted ß hereafter, may convey information about lunar paleomagnetism. Indeed, high ß values may point to more single domain like behavior (for a given paleofield) or to higher paleofields (for a given magnetic mineralogy).

The paleointensity of 23 selected samples measured in this study have already been determined in previous laboratory studies (part S8, Table S4). ß appears broadly correlated with the paleointensity (Figure 6). However, a trend line does not intercept at the origin (B,ß)=(0,0). Indeed probably because of secondary magnetization components, hardly any samples have ß below 1. Qualitatively, we estimate that ß values below 4 have no real paleointensity significance. Selecting samples with ß $\geq$4, and forcing the x-intercept of the linear fitting to ß=4, we have a relation B = 9.7 * (ß-4) (R^2=0.63) with B in µT and ß in A/m. This relation indicates that the overall ß dataset may be informative about the overall evolution of lunar paleointensities and allows using ß as a crude paleointensity proxy.

However, there are various reasons why ß may not be a good proxy for the paleointensity. First, the minerals that carry the magnetic susceptibility signal are not necessarily the same ones that carry the NRM. This may introduce a mineralogical bias in the interpretation. Unfortunately, the formation ages of the various lithologies are clustered in discrete and mostly non overlapping periods so that this lithological bias is difficult to circumvent. Second, it would be better to normalize NRM by ferromagnetic susceptibility only, since the paramagnetic minerals contribute to the susceptibility but not to the remanence. As we do not know the paramagnetic susceptiblity of most Apollo rocks, however, we chose not to apply a blanket correction to the susceptibility that may introduce an additional source of uncertainty. Third, we measured the total NRM of the samples without any magnetic cleaning. Therefore these rocks may be affected by secondary magnetizations (i.e., not acquired on the Moon) like viscous remanent magnetization (VRM) acquired during the ~50 years stay of the Apollo rocks in the geomagnetic field, but also by all magnetic contaminations that may have occurred at differents stages of the Apollo samples' history (during sampling on the Moon, in the return spacecraft, during cutting and processing at JSC). Regarding VRM, it is noteworthy that the studied samples were kept in a mumetal container in ambient field < 200 nT for at least 24 hours before their NRM was measured, allowing for relaxation of about 50% of a 50 year VRM assuming a similar acquisition and decay rate for VRM. As an example we measured in the laboratory (CEREGE) the NRM and the magnetic susceptibility of a small piece of sample 14169 (73 mg). The NRM (6.45 x 10^{-5} Am^2kg^{-1}) was measured using a SQUID cryogenic magnetometer and the susceptibility (2.34 x 10^{-6} m^3kg^{-1})

using a MFK1 instrument. The NRM was then stepwise demagnetized using alternating fields (AF). This particular sample has a large secondary component (possibly a VRM), removed between 2 mT and 6 mT AF (Figure 7a). As a consequence ß decreases rapidly during AF demagnetization and reaches much lower values than that obtained on the whole rock at LSLF (Figure 7b). This ß value of 16.5, measured on a 72.4 g sample, is clearly dominated by the secondary component of the sample. It is therefore hardly related to the high coercivity component of magnetization which would relate to the lunar surface field during the formation of this rock on the Moon. This effect can enhance ß for some samples with no relation to the paleofield intensity. Finally the possibility that the large block magnetic susceptibility is biased toward higher value by surface contamination and coating by regolith material may add another bias since this contamination will increase the magnetic susceptibility but not necessarily the bulk NRM.

A plot of ß as a function of time reveals different behaviors over the high-field epoch (between 4.25 and 3.56 Ga in literature) and weak-field epoch (after ~3.5 Ga) discussed above (Figure 8). There is more scatter in the high-field epoch with 7/40 samples with high ß value (ß > 10 A/m, including samples 14053 and 14305 with ß > 20 A/m) between 4 and 3 Ga (Figure 8). However, 23 samples, accounting for 64% of samples in this period, have low ß values (ß < 5 A/m). A majority of samples have ß < 5 A/m in the weak-field epoch (18/48 samples higher than 5 A/m) and only 1 sample has ß > 20 A/m (sample 12010 with ß = 25.2 A/m). A median value computed on a sliding window of 15 ß values (grey line in Figure 8) agrees qualitatively with the existence of the high-field and weak-field epochs. It is noteworthy that a significant fraction of samples from the high-field epoch have low ß values (23/40 with ß < 5 A/m). They may correspond to samples with low paleointensities, suggesting that the average field in the high field epoch may have been overestimated in previous studies because of the focus on highly magnetized samples. Alternatively they could correspond to samples whose original NRM has been partially or totally erased by a later process. Shock in particular is able to remagnetize rocks and in view of the low efficiency of shock magnetization compared to TRM (e.g., *Tikoo et al*., 2015), the result of shock remagnetization would be a drastic decrease of ß regardless of the intensity of the lunar surface field at the time of impact. Other explanation for low ß could be post NRM acquisition “cold” brecciation (without resetting of radiometric ages but clast-scale randomization of the NRM) and recent contamination by metal rich regolith.

With all these caveats in mind, the dataset presented in Figure 8 allows selecting samples for laboratory studies addressing specific questions about the lunar surface field evolution.

4. Conclusions

Using two portable instruments specifically designed for this project, we obtained magnetic susceptibility and NRM measurements on 154 and 123 Apollo whole samples, respectively. This dataset represents a significant increase in number (+52% for NRM and +64% for susceptibility) and in mass (80 kg against 20.5 g for the literature dataset) of the existing database of lunar magnetic properties.

Our lithology-averaged NRM values may be more representative of the large-scale magnetic parameters than the values measured on small samples usually well below 1 gram that appears overestimated by an average factor of ~2.7. The NRM values obtained in this work are therefore more suitable to model and interpret the lunar magnetic field anomalies. Conversely, our magnetic susceptibility estimates may be overestimated for some weakly magnetic lithologies because of coating by glass or regolith material on bulk samples. Overall, magnetic susceptibility is strongly controlled by lithology and is clearly enhanced by impact processing and associated incorporation of meteoritic metal.

The ratio of natural remanence and magnetic susceptibility may be used as a crude paleointensity proxy. Its overall evolution with time is coherent with the existence of the high field and weak field epochs defined in the literature. However our data raise the possibility that the paleointensity during the high field epoch may have been more variable and lower on average than previously suggested. Although this ratio cannot provide robust paleointensities, our dataset represents a valid tool to select samples of interest for detailed paleomagnetic laboratory study.

Acknowledgements

This work was funded by the Agence Nationale de la Recherche (project Maglune, ANR-14-CE33-0012) and the Programme National de Planétologie (INSU/CNES).

References

Buz, J., Weiss, B.P., Tikoo, S.M., Shuster, D.L., Gattacceca, J. and Grove T.L., 2015. Magnetism of a very young lunar glass. Journal of Geophysical Research: Planets 120 (1720-1735), doi:10.1002/2015JE004878.

Cournede, C., Gattacceca, J., and Rochette, P., 2012. Magnetic study of large Apollo samples: Possible evidence for an ancient centered dipolar field on the Moon. Earth and Planetary Science Letters 331-332 (31-42), doi:10.1016/j.epsl.2012.03.004.

Dolginov, S.S., Eroschenko, E.G., Zhuzgov. L.N., and Pushkov. N.V., 1966. Measurements in the vicinity of the Moon by the artificial satellite Luna 10. Dokl. Akad. Nauk SSSR 170 (574-577).

Dwyer, C.A., Stevenson, D.J., and Nimmo, F., 2011. A long-lived lunar dynamo driven by continuous mechanical stirring. Nature Letter 479 (212-214), doi:10.1038/nature10564.

Evans, A.J., Tikoo, S.M. and Andrews-Hanna, J.C., 2017. The case against an early lunar dynamo powered by core convection. Geophysical Research Letters 45 (98-107), doi: 10.1002/2017GL075441.

Fagan, A.L., Joy, K.H., Bogard, D.D. and Kring, D.A., 2014. Ages of globally distributed Lunar paleoregoliths and soils from 3.9 Ga to the present. Earth Moon Planets 112 (59-71), doi:10.1007/s11038-014-9437-7.

Fuller, M., and Cisowski, S.M., 1987. Lunar paleomagnetism. In: Jacobs, J.A. (Ed.), Geomagnetism. Academic Press, San Diego, CA, pp. 307–456.

Garrick-Bethell, I., Weiss, B.P., Shuster, D.L., and Buz, J., 2009. Early Lunar Magnetism. Science 323 (356), doi:10.1126/science.1166804.

Garrick-Bethell, I., Weiss, B.P., Shuster, D.L., Tikoo, S.M. and Tremblay, M.M., 2017. Further evidence for early lunar magnetism from troctolites 76535. Journal of Geophysical Research: Planets, 122 (76-93), doi:10.1002/2016JE005154.

Gattacceca, J., Eisenlohr, P. and Rochette, P., 2004. Calibration of *in situ* magnetic susceptibility measurements. Geophysics Journal Interiors 158 (42-49), doi: 10.1111/j.1365-246X.2004.02297.x.

Heiken, G.H., Vaniman, D.T. and French, B.M., 1991. Lunar source book, a user's guide to the moon. Cambridge university press. Lunar and Planetary Institue, 736p.

Hiesinger, H., Head III, J.W., Wolf, U., Jaumann, R. and Neukum, G., 2011. Ages and stratigraphy of lunar mare basalts: A synthesis. The Geological Society of America, Special paper 477 (1-51), doi:10.1130/2011.2477(01).

Laneuville, M., Wieczorek, M.A., Breuer, D., Aubert, J., Morard, G., and Rückriemen, T., 2014. A long-lived lunar dynamo powered by core crystallization. Earth and Planetary Science Letters 401 (251-260).

Lawrence, K., Johnson, C., Tauxe, L., and Gee, J., 2008. Lunar paleointensity measurements: Implications for lunar magnetic evolution. Physics of the Earth and Planetary Interiors 168 (71-87), doi:10.1016/j.pepi.2008.05.007.

Le Bars, M., Wieczorek, M.A., Karatekin, Ö., Cébron, D. and Laneuville, M., 2011. An impact-driven dynamo for the early Moon. Science Research Letter 479 (215-220), doi:10.1038/nature10565.

Macke, R.J., Kiefer, W.S., Britt, D.T., Consolmagno, G.J and Irving, A.J., 2014. New lunar sample density and magnetic susceptibility measurements. 45th Lunar and Planetary Science Conference, poster #1949.

Oliveira, J.S., Wieczorek, M.A. and Kletetschka, G., 2017. Iron abundances in lunar impact basin melt sheets from orbital magnetic field data. Journal of Geophysical Research: Planets 122 (12), 2429-2444.

Rochette, P., Gattacceca, J., Ivanov, A.V., Nazarov, M.A. and Bezaeva, N.S., 2010. Magnetic properties of lunar materials: Meteorites, Luna and Apollo returned samples. Earth and Planetary Science Letters 292 (383-391), doi:10.1016/j.epsl.2010.02.007.

Shea, E.K., Weiss, B.P., Cassata, W.S., Shuster, D.L., Tikoo, S.M., Gattacceca, J., Grove, T.L., and Fuller, M.D., 2012. A long-lived lunar core dynamo. Science 335 (453), doi: 10.1126/science.1215359.

Sonett, C.P., Colburn, D.S., Currie, R. G. and Mihalov. J.D., 1967. The geomagnetic tail, topology, reconnection and interaction with the Moon. Physics of the Magnetosphere (461-484).
Steiger, R.H. and Jäger, E., 1977. Subcommission of geochronology : Convention on the use of decay constants in geo- and cosmochronology. Earth and Planetary Science Letters 36 (359-362).
Suavet, C., Weiss, B.P., Cassata, W.S., Shuster, D.L., Gattacceca, J., Chan, L., Garrick-Bethell, I., Head, J.W., Grove, T.L., and Fuller, M.D., 2013. Persistence and origin of the lunar core dynamo. Earth, Atmospheric, and Planetary Sciences 110 (8453-8458).
Tikoo, S.M., Weiss, B.P., Buz, J., Lima, E.A., Shea, E.K., Melo, G., and Grove, T.L., 2012a. Magnetic fidelity of lunar samples and implications for an ancient core dynamo. Earth and Planetary Science Letters 337-338 (93-103).
Tikoo, S.M., Weiss, B.P., Cassata, W.S., Shuster, D.L., Gattacceca, J., Lima, E.A., Suavet, C., Nimmo, F., and Fuller, M.D., 2014. Decline of the lunar core dynamo. Earth and Planetary Science Letters 404 (89-97).
Tikoo, S.M., Gattacceca, J., Swanson-Hysell, N.L., Weiss, B.P., Suavet, C. and Cournède, C., 2015. Preservation and detectability of shock-induced magnetization. Journal of Geophysical Research: Planets 120 (1461-1475), doi:10.1002/2015JE004840.
Tikoo, S.M., Weiss, B.P., Shuster, D.L., Suavet, C., Wang, H., and Grove, T.L., 2017. A two-billion-year history for the lunar dynamo. Science Advances 3, e1700207.
Uehara, M., Gattacceca, J., Quesnel, Y., Lepaulard, C., Lima, E.A., Manfredi, M., and Rochette, P., 2017. A spinner magnetometer for large Apollo lunar samples. Review of Scientific Instruments 88 (104502).
Wang, H., Mighani, S., Weiss, B.P., Shuster, D.L., and Hodges, K.V., 2017. Lifetime of the lunar dynamo constrained by young Apollo returned breccias 15015 and 15465. Lunar and Planetary Science XLVIII.
Weiss, B.P., and Tikoo, S.M., 2014. The lunar dynamo. Science 346, 1246753, doi: 10.1126/science.1246753.

Figures and table captions

Figure 1: a) Distribution of the NRM intensities of the large Apollo samples measured in this study, grouped by lithology. b) Distribution of the magnetic susceptibility of the large Apollo samples measured in this study, grouped by lithology. Numbers of analysed samples are indicated for each lithology (number for NRM, number for susceptibility). Note the non-linear scales for both NRM and susceptibility.

Figure 2: a) NRM average values of small samples (literature data, with standard deviations) versus NRM average values of large samples (this study, with standard deviations) by lithology. b) Magnetic susceptibility average values of small samples (literature data, with standard deviations) versus magnetic susceptibility average values of large samples (this study, with standard deviations) by lithology. In both figures numbers in parentheses refer to the number of samples in our dataset and the literature dataset, respectively, and the light broken line is a 1:1 line. Literature data are listed in Table S2.

Figure 3: NRM intensities measured on small samples (literature data) versus NRM values of large intensities measured on large samples of the same rocks (this study). Box symbols connected by vertical lines are for rocks with several small sub-samples in the literature dataset. The error bars are smaller than the symbol size. Sample 15015 is not plotted due to anomalous results in the literature, but it is listed in Table S2, with all literature data.

Figure 4: Magnetic susceptibility of small samples (literature data) versus magnetic susceptibility values of large samples (this study, with error bars). Box symbols connected by vertical lines are for rocks with several sub-samples in the literature dataset. Samples 77135, 72275 and 60255 are not plotted due to anomalous results in the literature, but all literature data are listed in Table S2.

Figure 5: Magnetic susceptibility data measured with our custom made susceptibility meter (average sample mass 1130 g for this subset of samples) versus magnetic susceptibility measured using a SM30 susceptibility meter on different samples (with average mass 19 g) of the same Apollo rocks. The dotted line is a linear fit between the two dataset.

Figure 6: Paleointensity estimates (literature data, solid circles: paleointensity based on AF methods, open circles: paleointensity based on thermal methods) as a function of ß (with error bars). When several estimates are available the average paleointensity is used. When both AF- and thermal-based results are available, the AF-based result is used, except for recent result on 15015 that was obtained using oxygen fugacity controm (*Wang et al,*. 2017). The single pTRM result of Brechet 1974 for 74275 was not used. The shaded area corresponds to ß <4 (see section 3.3). Sample 14305 was not included in this plot because of its peculiar magnetic mineralogy (NRM being carried by cohenite; e.g *Cournède et al*., 2012) that sets it apart from all other Apollo samples. Paleointensities results from literature are listed Table S4.

Figure 7: Laboratory NRM measurements for Apollo rock 14169. a) Orthogonal projection plot for a 73 mg sub-sample. b) ß ($A.m^{-1}$) as a function of alternating field. The dashed line is the ß value for the 72.4 g block measured at JSC.

Figure 8: ß (with error bars) as a function of the age of studied rocks. Color-coding refers to lithology. The grey line corresponds to a sliding median, calculated on 15 successive ß values. The right axis indicates the approximate paleointensity for ß > 4 (broken line, see section 3.3 and fig. 6). The dark line corresponds to the literature limit (at 3.5 Ga) between the high and the weak field epoch.

Table 1: NRM and magnetic susceptibility sorted by lithology. N: number of reliable measurements (see text); No: number of samples studied in this work; S.D: standard deviation.

Physics of the Earth and Planetary Interiors

Table 1 for

A survey of the natural remanent magnetization and magnetic susceptibility of Apollo whole rocks

Camille Lepaulard[1], Jérôme Gattacceca[1], Minoru Uehara[1], Pierre Rochette[1], Yoann Quesnel[1], Robert J. Macke, S.J.[2], Walter Kiefer[3]

[1]Aix Marseille University, CNRS, IRD, Coll. France, INRA, CEREGE, Aix-en-Provence, France

[2]Vatican Observatory, Vatican City-State

[3]Lunar and Planetary Institute, Houston, Texas, USA

Corresponding author: Camille Lepaulard (lepaulard@cerege.fr)

Contents of this file

Table 1

Table 1 :

NRM and magnetic susceptibility sorted by lithology. N: number of reliable measurements (see text); No: number of samples studied in this work; S.D: standard deviation.

Lithology	NRM mean ($10^{-6}Am^2kg^{-1}$)	NRM S.D ($10^{-6}Am^2kg^{-1}$)	NRM median ($10^{-6}Am^2kg^{-1}$)	NRM minimum ($10^{-6}Am^2kg^{-1}$)	NRM maximum ($10^{-6}Am^2kg^{-1}$)	N/No	χ mean ($10^{-6}m^3kg^{-1}$)	χ S.D ($10^{-6}m^3kg^{-1}$)	χ median ($10^{-6}m^3kg^{-1}$)	χ minimum ($10^{-6}m^3kg^{-1}$)	χ maximum ($10^{-6}m^3kg^{-1}$)	N/No
Regolith breccia	75.20	63.06	55.91	4.83	225.6	44 / 50	19.11	16.65	13.89	2.65	73.8	44 / 50
Impact melt breccia	20.72	25.67	9.24	1.30	85.6	39 / 52	4.11	2.78	3.69	0.15	11.5	49 / 52
Dimict breccia	32.44	41.99	11.09	2.71	104.9	4 / 5	6.10	3.81	1.57	2.03	10.6	5 / 5
Impact melt rocks	33.54	31.00	19.07	2.45	74.1	5 / 6	6.07	4.78	4.32	1.16	13.1	5 / 6
Basalts	18.87	43.36	8.20	1.25	243.4	29 / 40	1.81	1.48	1.41	0.64	9.8	39 / 40
Feldspathic rocks	4.75	2.92	4.75	1.83	7.7	2 / 8	1.91	2.35	1.15	0.020	7.8	8 / 8
					Total	**123 / 161**					**Total**	**154 / 161**
Literature data												
Regolith breccia	199.79	328.06	69.50	31.00	1000.0	7	23.72	18.58	16.46	4.17	75.9	14
Impact melt breccia	44.55	46.96	23.20	1.80	147.0	24	7.22	11.63	3.13	0.28	45.7	24
Dimict breccia	80.50	7.50	80.50	73.00	88.0	2	-	-	-	-	-	0
Impact melt rocks	13.50	13.14	9.00	2.00	34.0	4	6.02	4.40	4.30	0.72	12.3	8
Basalts	37.24	70.86	15.85	0.54	500.0	61	1.59	1.60	1.10	0.41	9.8	48
Feldspathic rocks	6.05	8.90	1.04	0.17	30.2	11	2.04	5.02	0.041	0.0016	17.8	11
					Total	**109**					**Total**	**105**

A survey of the natural remanent magnetization and magnetic susceptibility of Apollo whole rocks

Camille Lepaulard[1], Jérôme Gattacceca[1], Minoru Uehara[1], Pierre Rochette[1], Yoann Quesnel[1], Robert J. Macke, S.J.[2], Walter Kiefer[3]

[1]Aix Marseille University, CNRS, IRD, Coll. France, INRA, CEREGE, Aix-en-Provence, France

[2]Vatican Observatory, Vatican City-State

[3]Lunar and Planetary Institute, Houston, Texas, USA

Corresponding author: Camille Lepaulard (lepaulard@cerege.fr)

Highlights

- We measured the natural remanence and magnetic susceptibility of 161 large (mean mass 500g) Apollo lunar samples in the LSLF (Houston)
- Magnetic properties are primarily controlled by impact processing
- The ratio of remanence to susceptibility can be used for sample selection for laboratory study, and is a crude proxy to paleointensity

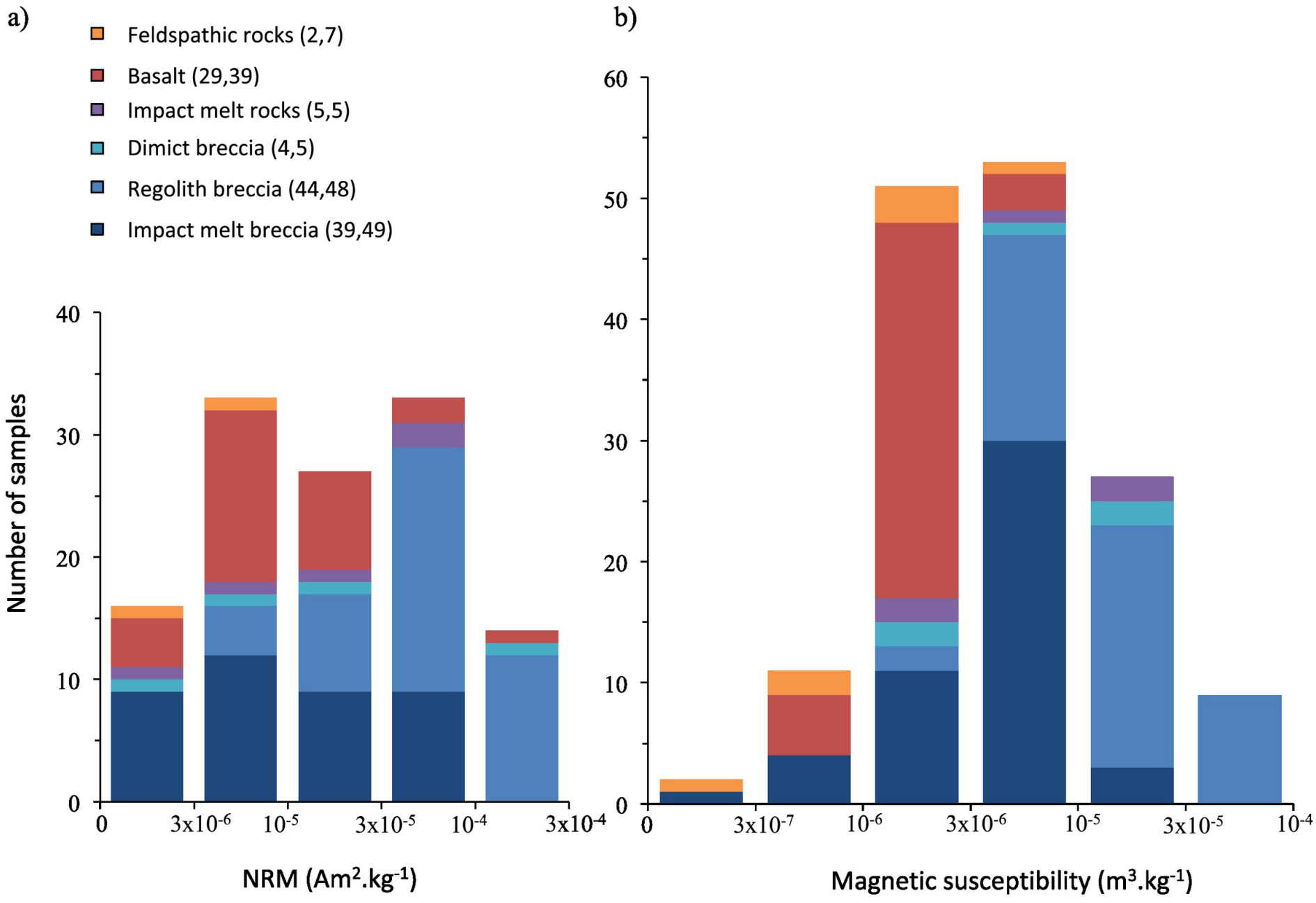
a)
b)
Feldspathic rocks (2,7)
Basalt (29,39)
Impact melt rocks (5,5)
Dimict breccia (4,5)
Regolith breccia (44,48)
Impact melt breccia (39,49)
Number of samples
0
10
20
30
40
50
60
0
3x10-6
10-5
3x10-5
10-4
3x10-4
NRM (Am2.kg-1)
0
3x10-7
10-6
3x10-6
10-5
3x10-5
10-4
Magnetic susceptibility (m3.kg-1)

Figure 1

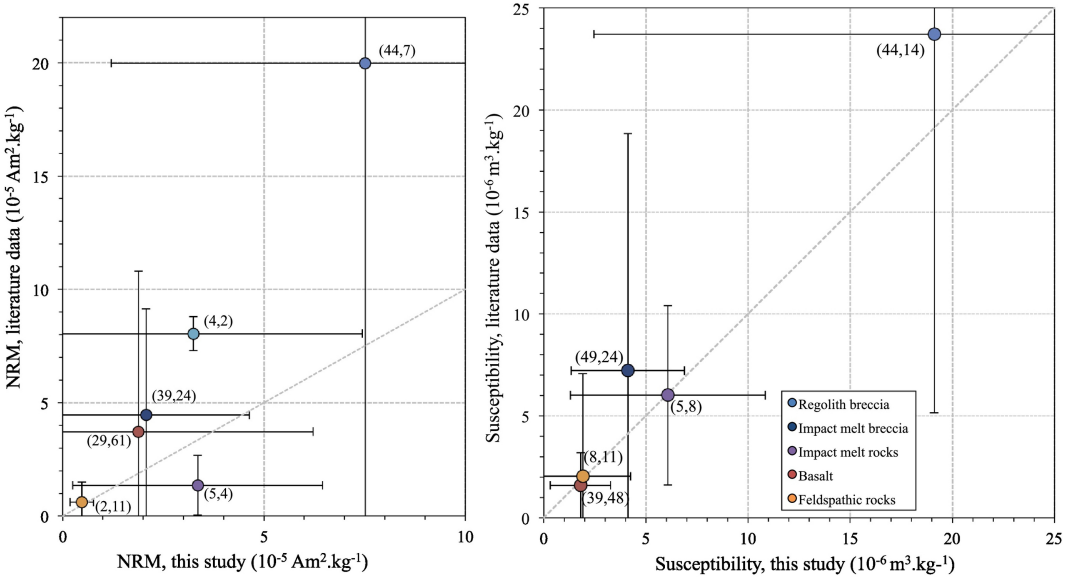
NRM, literature data (10^{-5} Am^2.kg^{-1})
NRM, this study (10^{-5} Am^2.kg^{-1})
(44,7)
(4,2)
(39,24)
(29,61)
(5,4)
(2,11)
Susceptibility, literature data (10^{-6} m^3.kg^{-1})
Susceptibility, this study (10^{-6} m^3.kg^{-1})
(44,14)
(49,24)
(5,8)
(8,11)
(39,48)
Regolith breccia
Impact melt breccia
Impact melt rocks
Basalt
Feldspathic rocks

Figure 2

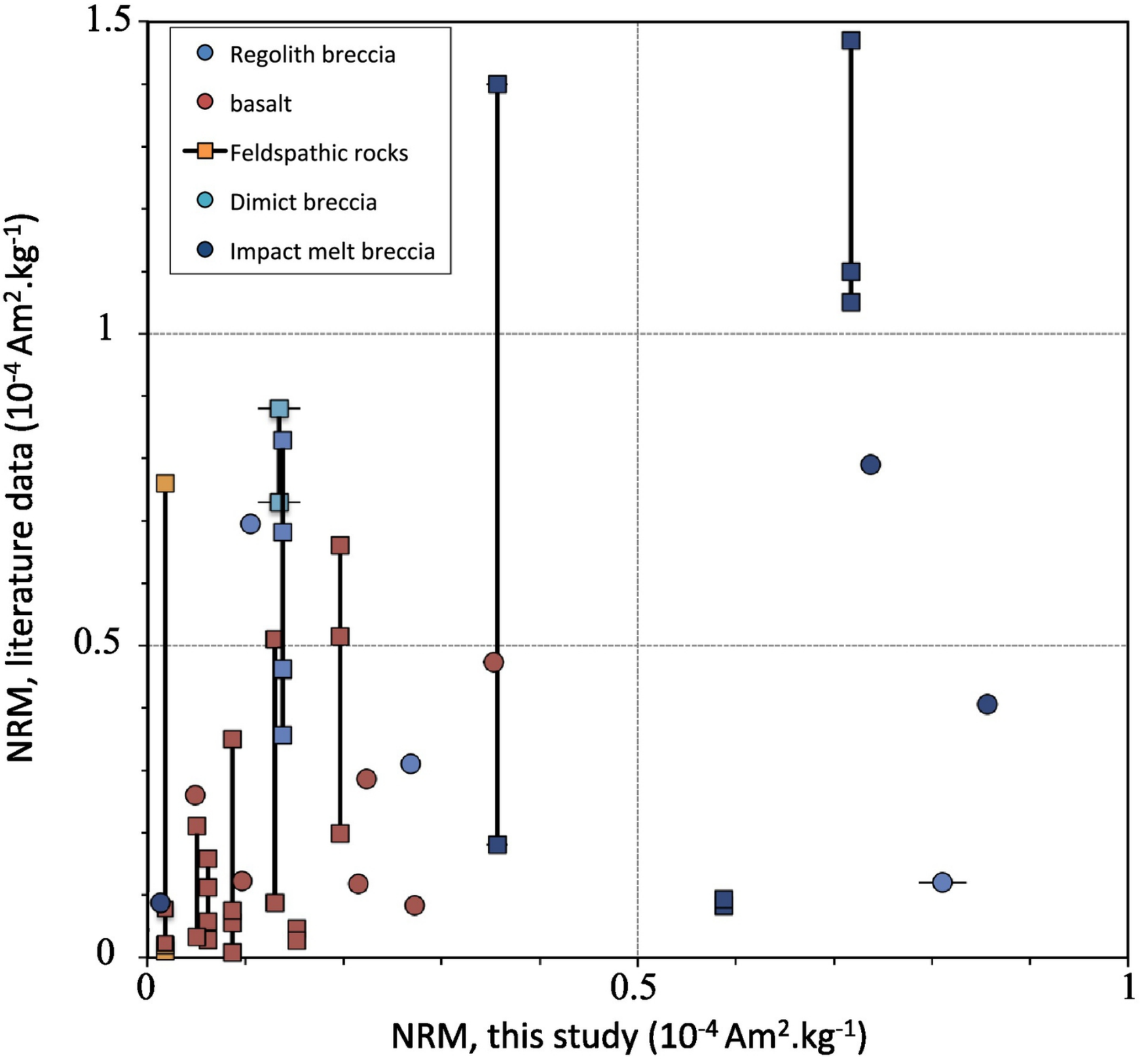
Regolith breccia
basalt
Feldspathic rocks
Dimict breccia
Impact melt breccia
NRM, literature data (10-4 Am2.kg-1)
NRM, this study (10-4 Am2.kg-1)
0
0.5
1
1.5
0
0.5
1

Figure 3

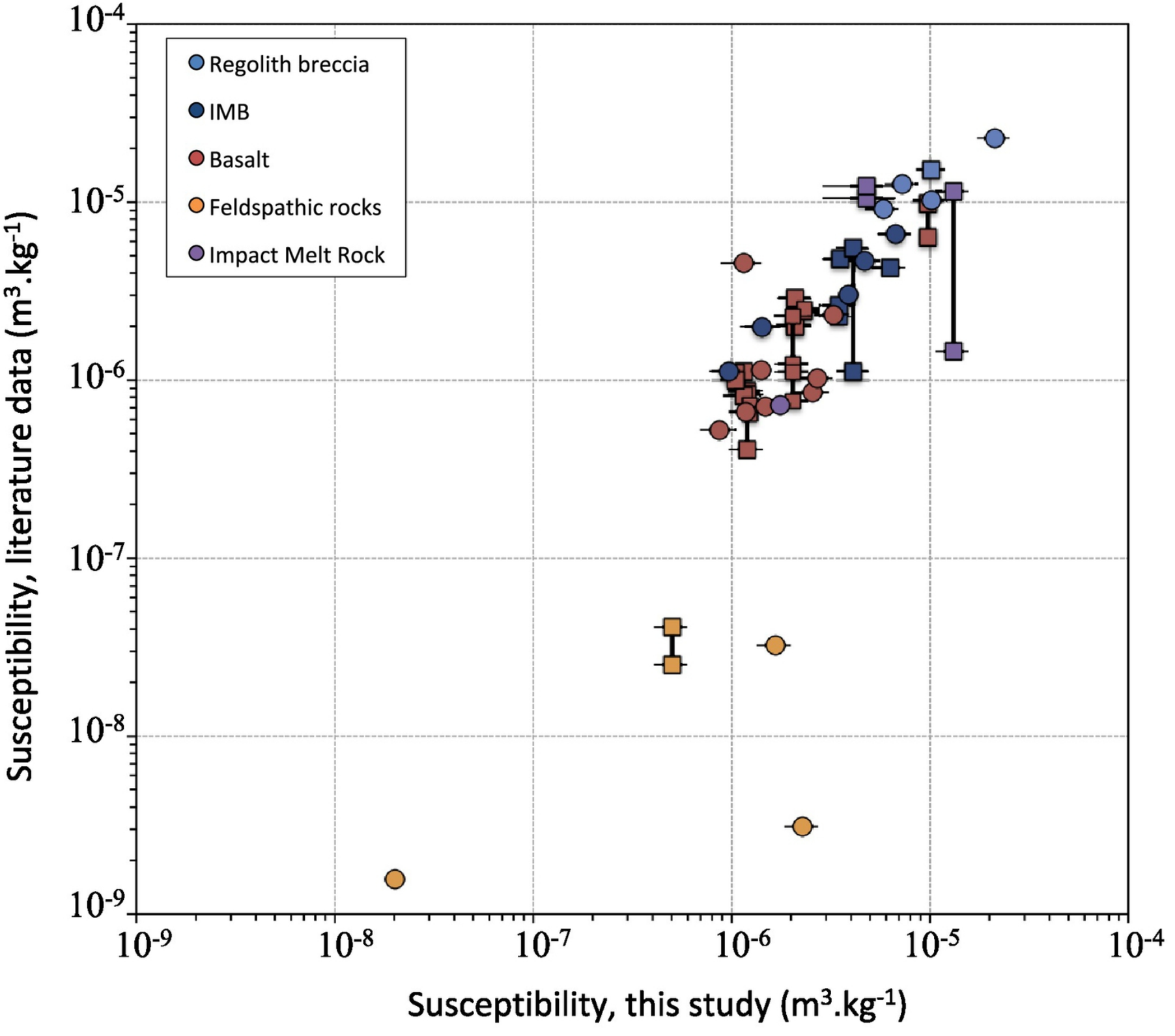
Regolith breccia
IMB
Basalt
Feldspathic rocks
Impact Melt Rock
Susceptibility, literature data (m³.kg⁻¹)
Susceptibility, this study (m³.kg⁻¹)
10⁻⁴
10⁻⁵
10⁻⁶
10⁻⁷
10⁻⁸
10⁻⁹

Figure 4

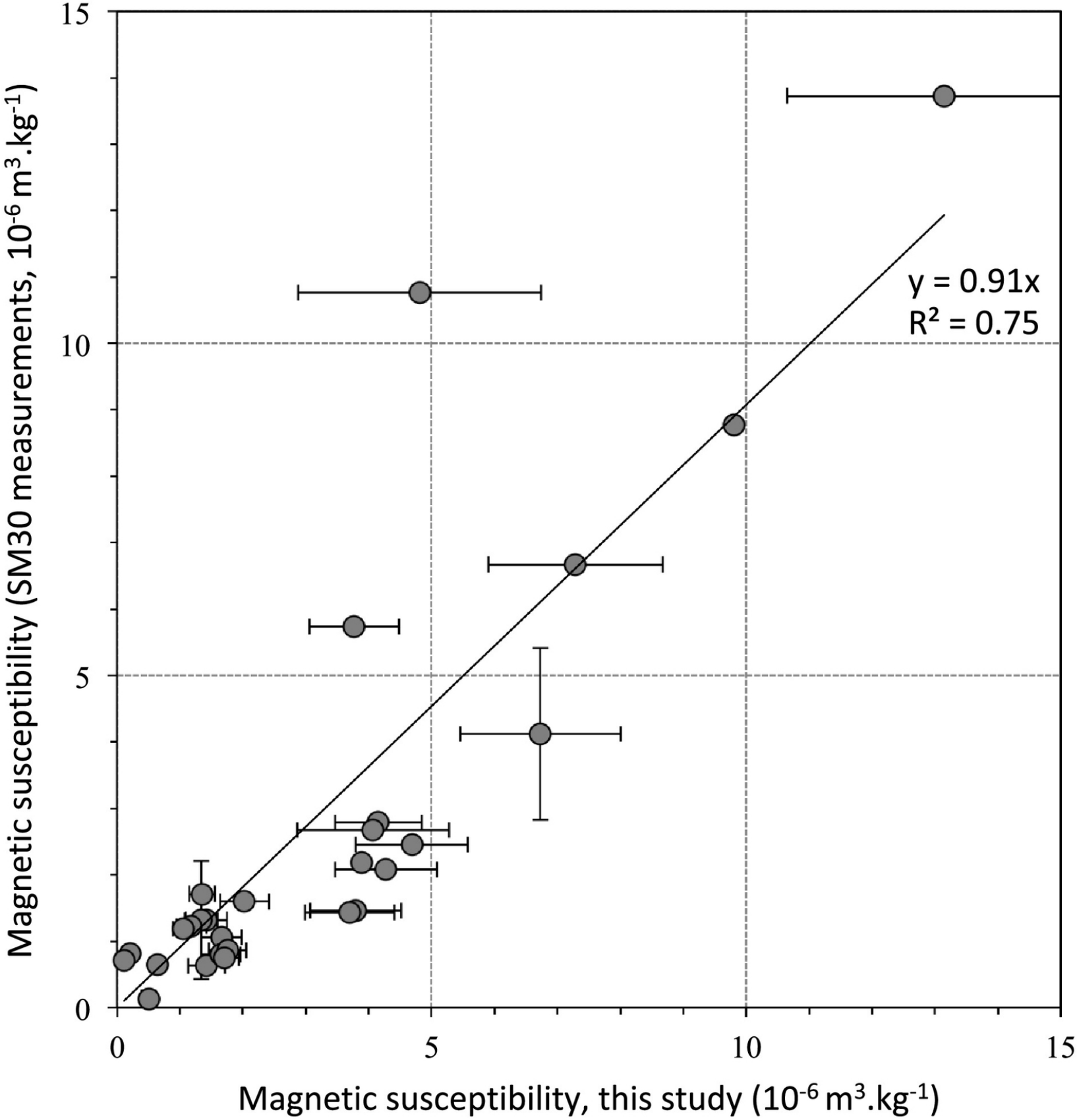
15
10
5
0
0
5
10
15
y = 0.91x
R² = 0.75
Magnetic susceptibility (SM30 measurements, 10-6 m3.kg-1)
Magnetic susceptibility, this study (10-6 m3.kg-1)

Figure 5

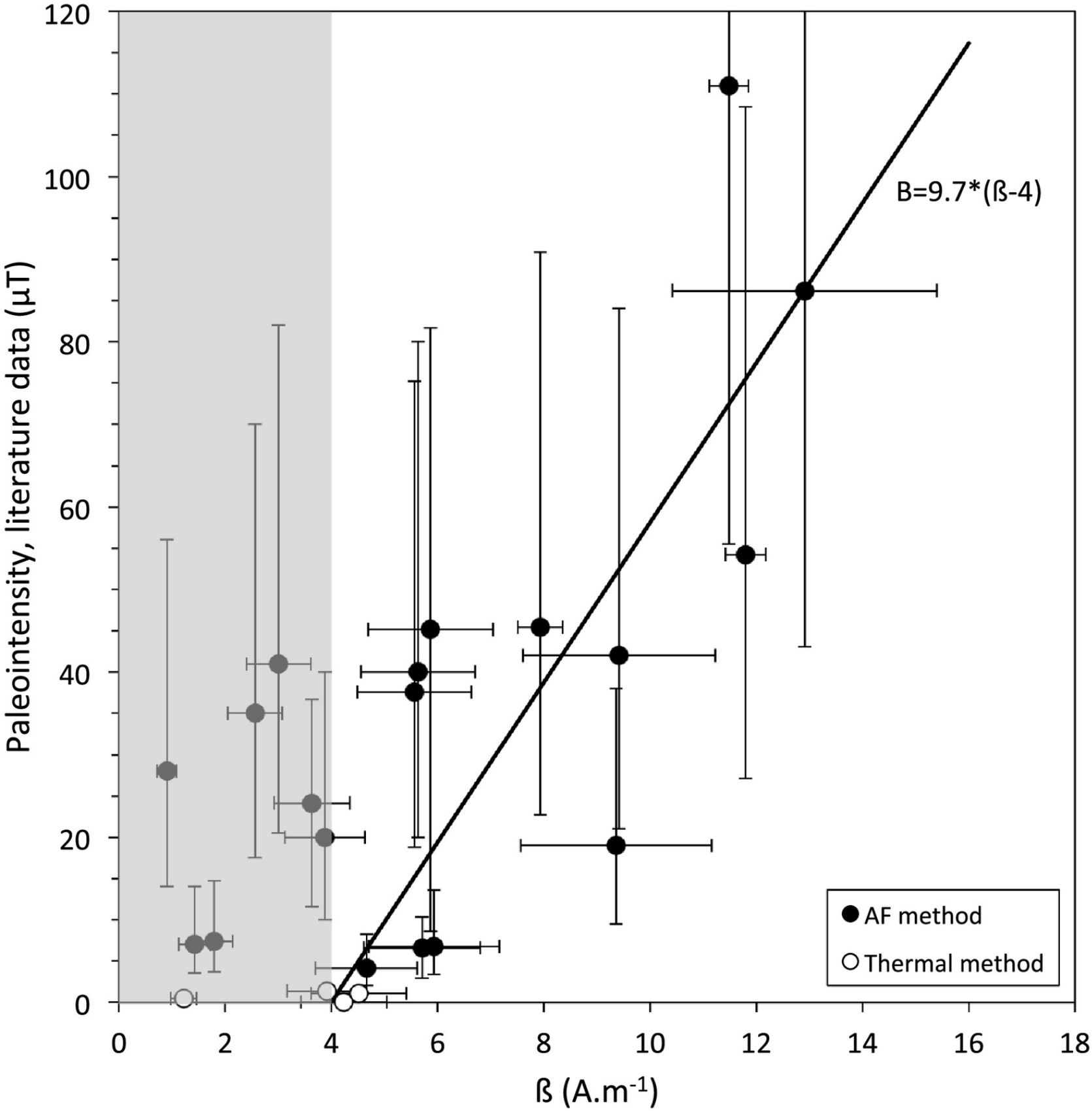
120
100
80
60
40
20
0
Paleointensity, literature data (µT)
0
2
4
6
8
10
12
14
16
18
ß (A.m-1)
B=9.7*(ß-4)
AF method
Thermal method

Figure 6

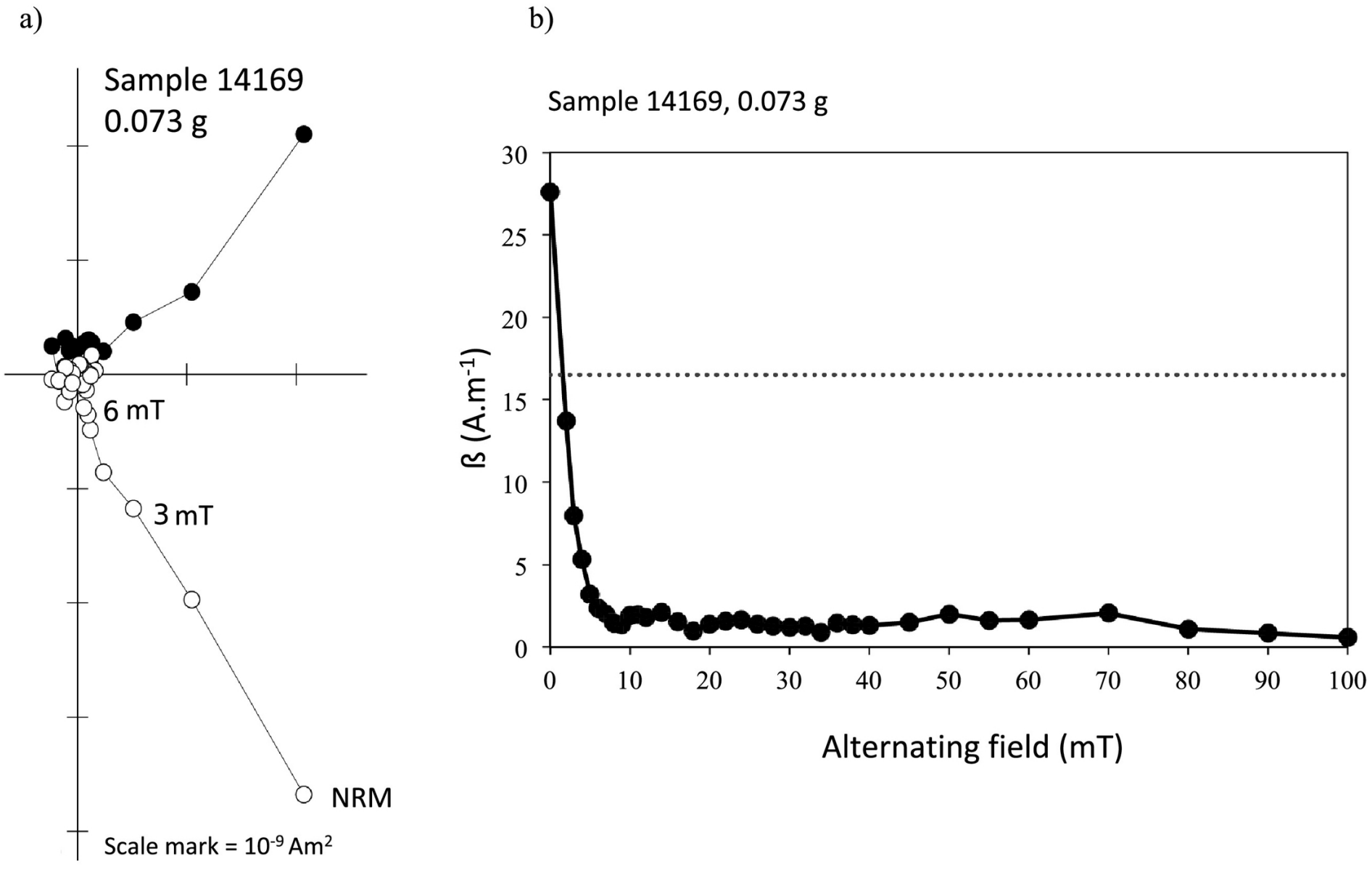
a)
Sample 14169
0.073 g
6 mT
3 mT
NRM
Scale mark = 10-9 Am2
b)
Sample 14169, 0.073 g
ß (A.m-1)
30
25
20
15
10
5
0
0
10
20
30
40
50
60
70
80
90
100
Alternating field (mT)

Figure 7

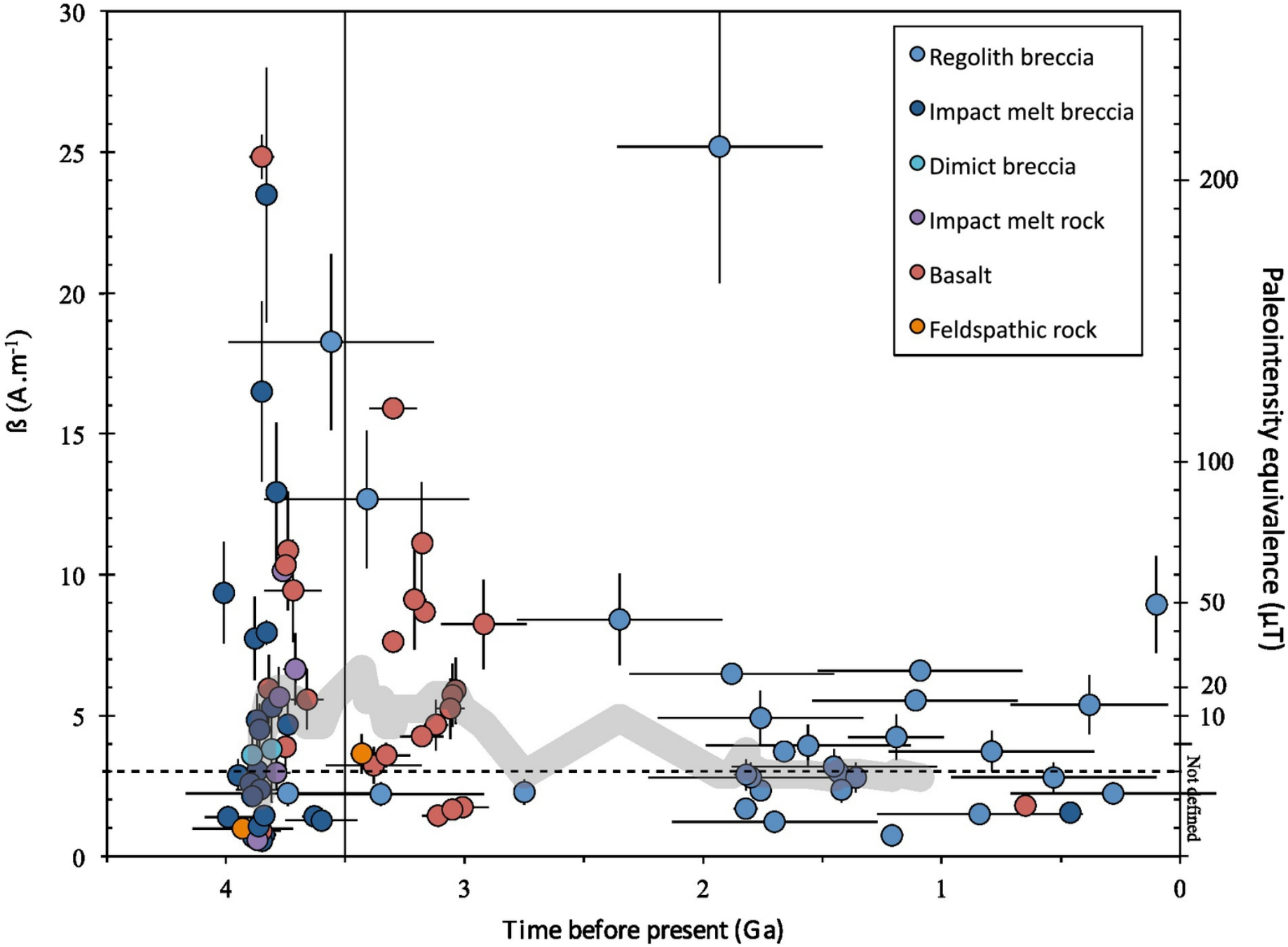
Regolith breccia
Impact melt breccia
Dimict breccia
Impact melt rock
Basalt
Feldspathic rock
ß (A.m-1)
Paleointensity equivalence (µT)
Time before present (Ga)
Not defined
30
25
20
15
10
5
0
200
100
50
20
10
4
3
2
1
0

Figure 8